

Supporting Information

Taking Orders from Light: Photo-Switchable Working/Inactive Smart Surfaces for Protein and Cell Adhesion

Junji Zhang,* Wenjing Ma, Xiao-Peng He,* He Tian

Key Laboratory for Advanced Materials & Institute of Fine Chemicals, School of Chemistry and Molecular Engineering, East China University of Science and Technology, 130 Meilong Rd., Shanghai 200237, P. R. China

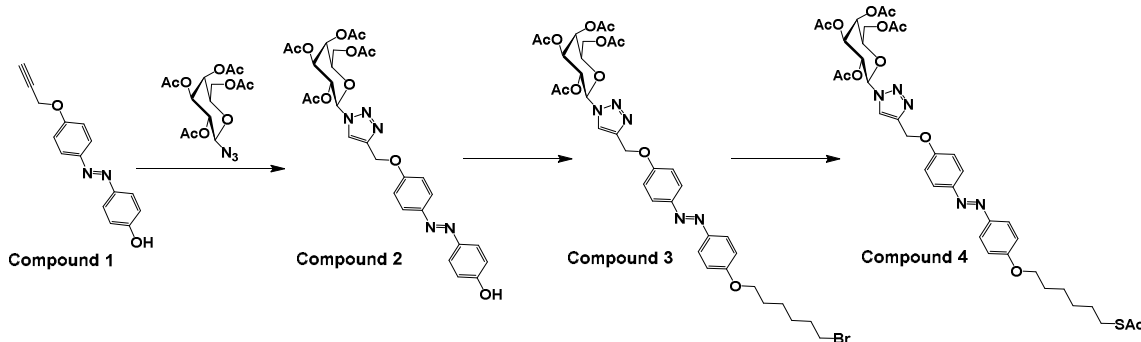
*Corresponding Authors

zhangjunji@ecust.edu.cn (J. Zhang)

xphe@ecust.edu.cn (X.-P. He)

S1. Synthesis of Monosaccharide-Azobenzene Derivatives

Azobenzene derivatives (compound 1 and 1') were synthesized according to previously reported work.¹⁻²



Scheme S1. Synthesis of acetylated galactose-azobenzene thiol precursor.
(E-(4'-Hydroxyphenylazo)phenyl)-1 methoxy-1,2,3-triazol-1-yl)2,3,4,6-tetra-O-acetyl-β-D-galactopyranoside (compound 2)

To a solution of the azobenzene derivative 1 (400 mg, 1.59 mmol) and the galactosyl donor (373 mg, 1.90 mmol) in CH₂Cl₂ (7 mL), CuSO₄ aqueous solution (1.5 mL, 3.18 mmol), L-ascorbic acid sodium aqueous solution (1.5 mL, 6.36 mmol) was added at the same time. The solution was stirred at room temperature overnight. The mixture was concentrated under reduced pressure to get the crude product which after purification by column chromatography (cyclohexane/ethyl acetate 6:4) gave the desired compound 2 as a yellow crystalline solid (696 mg, 70 %).

¹H NMR(400 MHz, CDCl₃): δ=7.97(s, 1H), 7.84(d, J=8.8Hz, 2H), 7.79(d, J=8.8Hz, 2H), 7.05(d, J=9.0Hz, 2H), 6.94(d, J=8.8Hz, 2H), 5.57(s, 2H), 5.29(s, 1H), 5.27(m, 3H), 4.22(m, 3H), 2.23(s, 3H), 2.05(s, 3H), 2.02(s, 3H), 1.88(s, 3H). TOF MS ES⁺ m/z: [M+1]⁺ calcd. for 625.2020, found 625.2012.

(E-(4-(4'-Bromohexylphenylazo)phenyl)-1 methoxy-1,2,3-triazol-1-yl)methyl 2,3,4,6-tetra-O-acetyl-β-D-galactopyranoside (compound 3)

To a solution of acetyl-protected galactoside 2 (500 mg, 0.80 mmol), 6-bromo-1-hexanol (432 mg, 2.40 mmol), triphenylphosphine (629 mg, 2.40 mmol) in dry THF (10 mL), DEAD (418 mg, 2.40 mmol) were added under N₂ atmosphere and the mixture was stirred at 0 °C for 1 h. Then, the reaction mixture was allowed to warm to room temperature and was stirred for another 5 h. The reaction mixture was evaporated to dryness and the crude product was purified by column chromatography (cyclohexane/ethyl acetate 3:2) to give compound 3 as a yellow solid (425 mg,

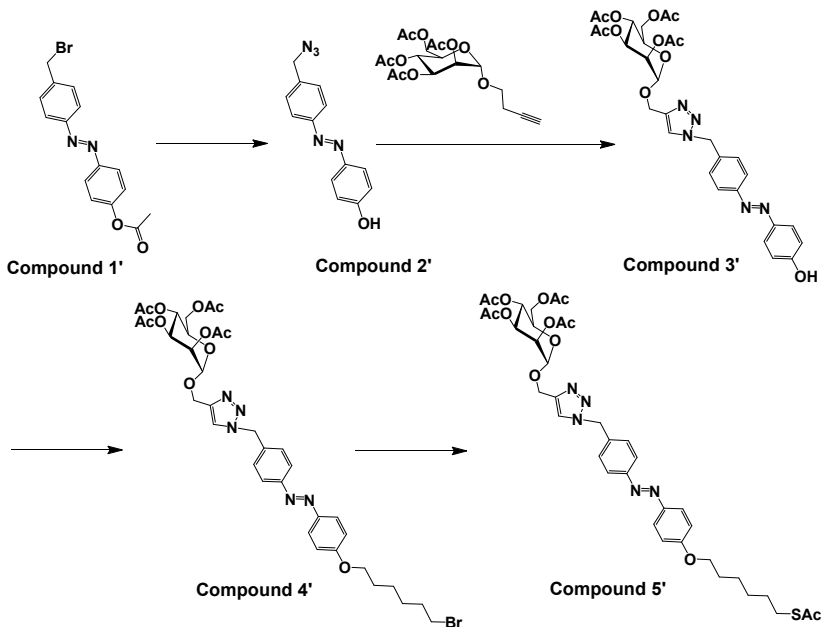
67.5%).

¹H NMR (400 MHz, CDCl₃): δ=7.89(d, J=7.88 Hz, 2H), 7.86(d, J=7.6 Hz, 2H), 7.52(s, 1H), 7.40(d, J=7.6 Hz, 2H), 7.00(d, J=8.8 Hz, 2H), 5.59(s, 2H), 5.39(d, J=3.6Hz, 1H), 5.20(t, J=9.6Hz, J=8.8Hz, 1H), 4.9(m, 2H), 4.82(d, J=12.4Hz, 1H), 4.04(t, J=6.4Hz, J=6.4Hz, 2H), 3.95(t, J=6.8Hz, J=6.4Hz, 1H), 3.43(t, J=7.2Hz, J=5.6Hz, 2H), 2.13(s, 3H), 2.04(s, 3H), 1.96(s, 3H), 1.88(s, 3H), 1.83(br, 2H), 1.52(br, 4H), 1.26(br, 2H). TOF MS ES⁺ m/z: [M+1]⁺ calcd. for 787.2064, found 787.2055.

(E-(4-(4'-Acetylthiohexylphenylazo)phenyl)-1 methoxy-1,2,3,-triazol-1-yl)methyl 2,3,4,6-tetra-O-acetyl-β-D- galactopyranoside (compound 4)

A mixture of the alkyl bromide 3 (300 mg, 0.38 mmol) and KSAc (52.2mg, 0.46 mmol) in DMF (5 mL) was stirred at room temperature overnight. Then, the reaction mixture was diluted with diethyl ether (100 mL) and the combined organic phase was washed with water (2×25 mL) and dried over MgSO₄. After filtration and the filtrate was evaporated to obtain the crude product, which was purified by column chromatography (cyclohexane/ethyl acetate 3:2) to yield compound 4 as a yellow solid (262 mg, 88 %).

¹H NMR(400 MHz, CDCl₃): δ=7.88(d, J=8.8Hz, 2H), 7.86(d, J=8.0, 2H), 7.52(s, 1H), 7.40(d, J=8.4Hz, 2H), 6.99(d, J=8.8Hz, 2H), 5.59(s, 2H), 5.38(d, J=3.4Hz, 1H), 5.20(m, 1H), 4.98(m, 1H), 4.82(d, J=12.8, 1H), 4.65(d, J=8.0, 1H), 4.14(d, J=6.4Hz, 2H), 4.03(t, J=6.4Hz, J=6.4Hz, 2H), 2.88(t, J=7.6Hz, J=7.2Hz, 2H), 2.32(s,3H), 2.13(s, 3H), 2.04(s,3H), 1.96(s, 3H), 1.87(m, 2H), 1.62(m, 2H), 1.47(m, 4H). ¹³C NMR (101 MHz, CDCl₃) δ 194.9 , 170.2 , 161.6 , 149.7 , 144.3 , 142.3 , 138.4 , 123.6 , 122.9 , 128.3 , 114.7 , 106.3 , 74.8 , 72.0 , 70.7 , 69.3 , 68.7 , 62.5 , 62.7 , 57.3 , 32.5 , 30.5 , 29.6 , 29.2 , 28.7 , 25.6 , 21 , 20.7. TOF MS ES⁺ m/z: [M+1]⁺ calcd. for 783.2785, found 783.2779.



Scheme S2. Synthesis of acetylated mannose-azobenzene thiol precursor.

(E-(4-(4'-Hydroxyphenylazo)phenyl)-1 methyl -2,3,4-triazol-1-yl - methyl) 2,3,4,6-tetra-O-acetyl- α -D-mannopyranoside (compound 3')

A solution of compound 1 (300 mg, 0.90 mmol) and NaN_3 (129 mg, 1.98 mmol) in acetonitrile: H_2O (v:v = 9:1, 5mL) was heated at 80 °C overnight. After cooled to room temperature, the reaction mixture was washed with H_2O and dried over Na_2SO_4 . After concentrated under vacuum, the corresponding azide (compound 2') was obtained and was used without further purification.

To a solution of the azobenzene derivative compound 2' (183 mg, 0.63 mmol) and the mannosyl donor (300 mg, 0.75 mmol) in CH_2Cl_2 (5 mL), CuSO_4 (1 mL, 1.24 mmol) and L-ascorbic acid sodium in aqueous solution (1 mL, 2.48 mmol) were added at the same time. The mixture was stirred at room temperature overnight. After filtration, the filtrate was concentrated under reduced pressure to get the crude product. Purification by column chromatography (cyclohexane/ethyl acetate 6:4) gave the desired compound 3' as a yellow crystalline solid (310 mg, 79 %).

^1H NMR(400 MHz, CDCl_3): δ =7.88(d, $J=3.6\text{Hz}$, 2H), 7.86(d, $J=4.2\text{Hz}$, 2H), 7.56(s, 1H), 7.43(d, $J=8.4\text{Hz}$, 2H), 6.95(d, $J=8.8\text{Hz}$, 2H), 5.62(s, 2H), 5.23(m, 1H), 4.95(d, $J=1.28$, 1H), 5.30(s, 2H), 5.23(m, 1H), 4.95(d, $J=1.28\text{Hz}$, 1H), 4.86(d, $J=12.4\text{Hz}$, 1H), 4.67(d, $J=12.4$, 1H), 4.29(dd, $J=5.2\text{Hz}$, $J=5.2\text{Hz}$, 1H), 4.06(s, 1H), 2.15(s, 3H), 2.11(s, 3H), 2.03(s, 3H), 1.97(s, 3H). TOF MS ES⁺ m/z: $[\text{M}+1]^+$ calcd. for 639.2177, found 639.2166.

(E-(4-(4'-Bromohexylphenylazo)phenyl)-1 methyl -2,3,4-triazol-1-yl - methyl)
S-4

2,3,4,6-tetra-O-acetyl- α -D-mannopyranoside (compound 4')

To a solution of acetyl-protected mannose 3' (200 mg, 0.32 mmol) and 6-bromo-1-hexanol (174 mg, 0.96 mmol), triphenylphosphine (252 mg, 0.96 mmol) in dry THF (6 mL), DEAD (167 mg, 0.96 mmol) was added at under N₂ atmosphere and the mixture was stirred at 0 °C for 1 h. Then, the reaction mixture was allowed to warm to room temperature and was stirred for another 5 h. The reaction mixture was evaporated to dryness and the crude product was purified by column chromatography (cyclohexane/ethyl acetate 3:2) to give compound 4' as a yellow solid (176 mg, 68.4%).

¹H NMR(400 MHz, CDCl₃): δ=7.89(d, J=8.8Hz, 2H), 7.88(d, J=8.0Hz, 2H), 7.56(s, 1H), 7.42(d, J=8.4Hz, 2H), 7.00(d, J=8.8Hz, 2H), 5.61(s, 2H), 5.30(s, 2H), 5.23(m, 1H), 4.97(d, J=1.28Hz, 1H), 4.95(m, 1H), 4.86(d, J=12.4Hz, 1H), 4.84(d, J=12.4Hz, 1H), 4.67(d, J=12.4Hz, 1H), 4.29(dd, J=5.2Hz, J=5.2Hz, 1H), 4.07(t, J=7.0Hz, J=7.0Hz, 2H), 3.43(t, J=6.8Hz, J=6.8Hz, 2H), 2.14(s, 3H), 2.10(s, 3H), 2.02(s, 3H), 1.97(s, 3H), 1.87(m, 4H), 1.53(dr, 4H). TOF MS ES⁺ m/z: [M+Na]⁺ calcd. for 801.2221, found 824.2142.

(E-(4'-Acetylthiohexylphenylazo)phenyl)-1 methyl -1,2,3-triazol-1-yl - methyl 2,3,4,6-tetra-O-acetyl- α -D-mannopyranoside (compound 5')

A mixture of the alkyl bromide 4 (150 mg, 0.18 mmol) and KSAc (25 mg, 0.22 mmol) in DMF (5 mL) was stirred at RT overnight. Then, the reaction mixture was diluted with diethyl ether (100 mL) and the combined organic phase was washed with water (2×25 mL) and dried over MgSO₄. After the filtration, the filtrate was evaporated to obtain the crude product, which was further purified by column chromatography (cyclohexane/ethyl acetate 3:2) to yield the compound 5' as a yellow solid (262 mg, 0.37 mmol, 88 %).

¹H NMR(400 MHz, CDCl₃) δ=7.83(d, J=7.2, 2H), 7.81(d, J=7.6, 2H), 7.48(s, 1H), 7.35(d, J=8.4Hz, 2H), 6.92(d, 8.8Hz, 2H), 5.54(s, 2H), 5.22(s, 2H), 5.15(dr, 1H), 5.00(m, 2H), 4.87(d, J=1.48Hz, 1H), 4.76(d, J=12.4Hz, 1Hz), 4.60(d, J=12.4Hz, 1H), 4.21(dd, J=5.2Hz, J=5.2Hz, 1H), 3.93(t, J=7.0Hz, J=7.0Hz, 2H), 2.82(t, J=7.2Hz, J=7.2Hz, 2H), 2.26(s, 3H), 2.07(s, 3H), 2.04(s, 3H), 1.96(s, 3H), 1.90(s, 3H), 1.56(m, 4H), 1.41(m, 4H). ¹³C NMR (101 MHz, CDCl₃) δ 169.9 , 169.7 , 160.9 , 151.7 , 145.7 , 143.4 , 127.9 , 127.6 , 123.9 , 122.3 , 121.9 , 113.7 , 95.7 , 69.4 , 67.9 , 67.7 , 67.1 , 65.0 , 61.9 , 61.7 , 61.3 , 60.1 , 52.9 , 29.6 , 28.7 , 28.4 , 27.9 , 27.4 , 24.5. TOF MS ES⁺ m/z: [M+1]⁺ calcd. for 797.2942, found 797.2922.

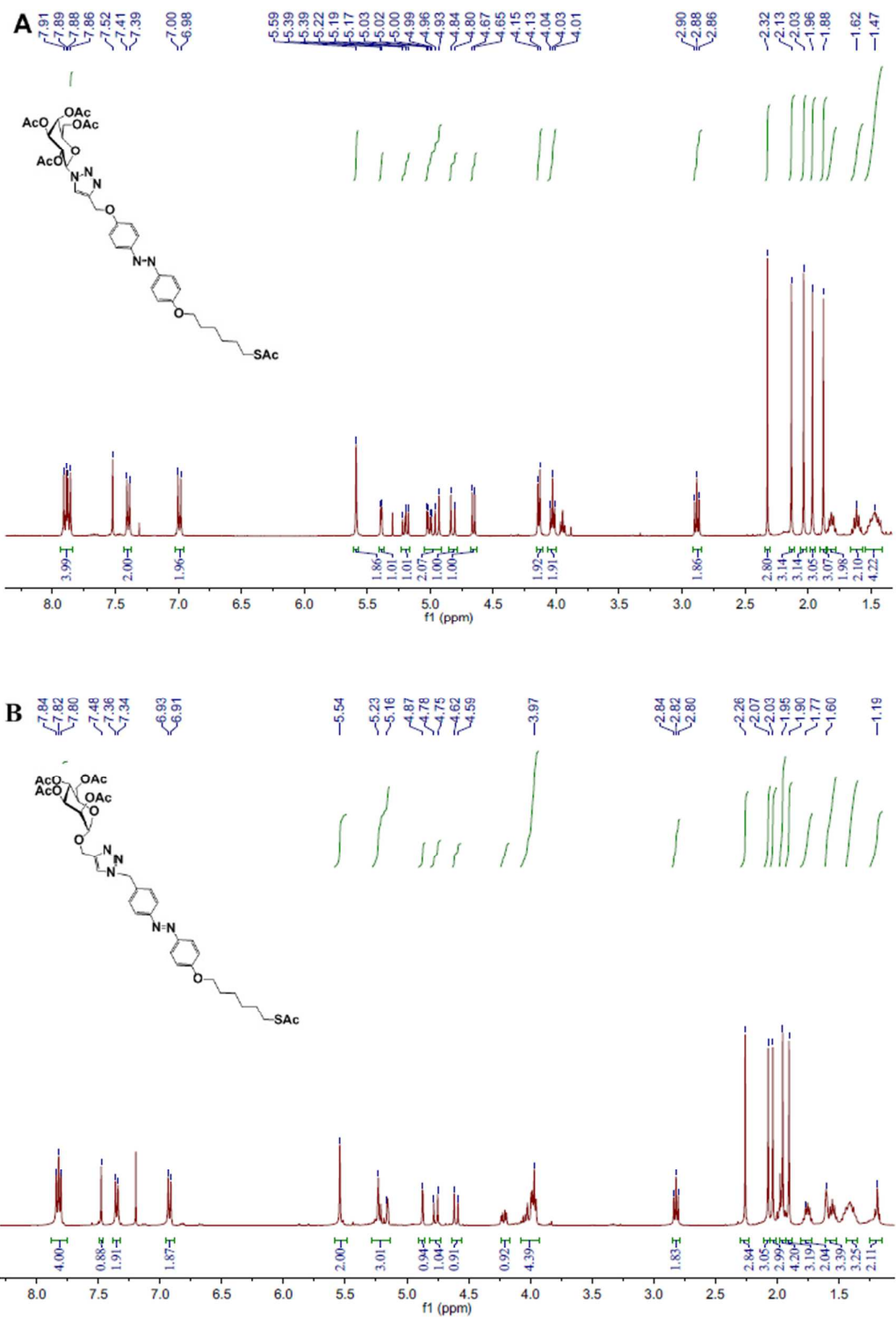


Figure S1. ^1H NMR spectra of (A) Compound 4 and (B) Compound 5'.

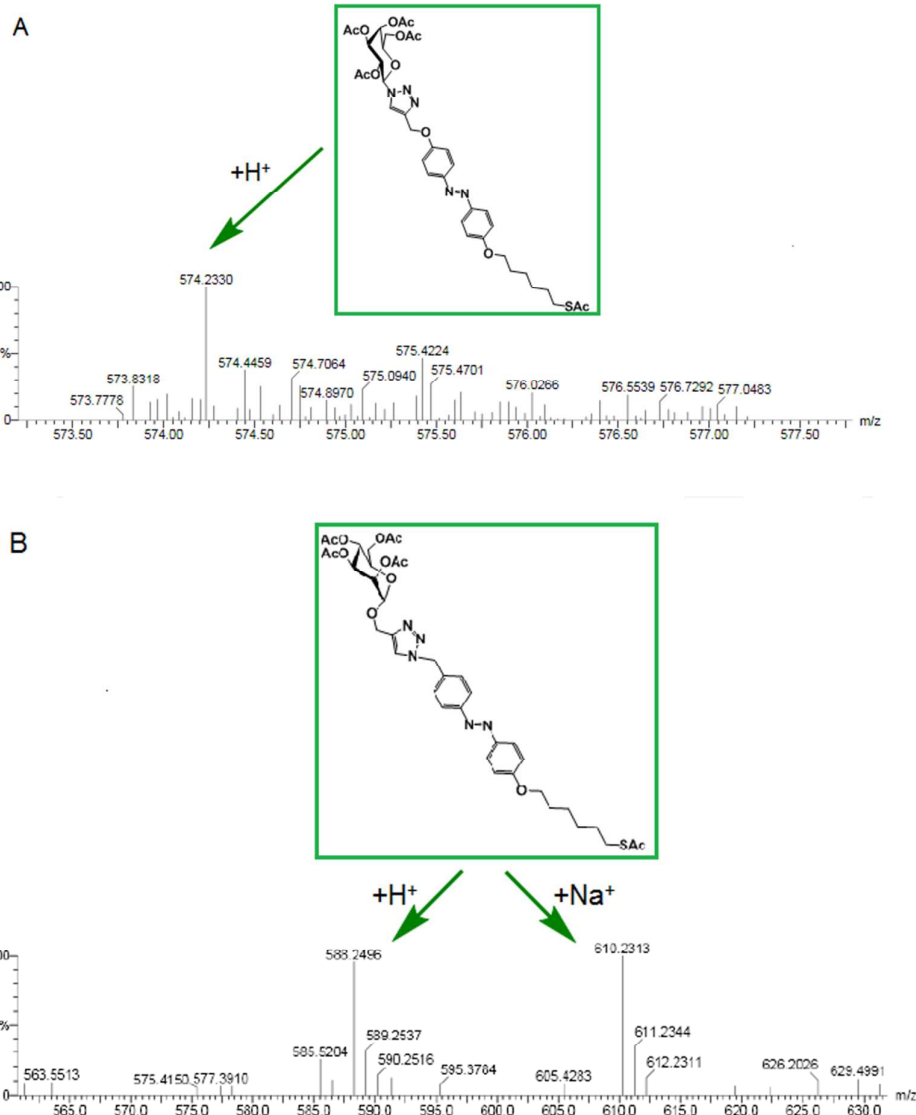


Figure S2. TOF MS ES⁺ spectra of (A) *trans*-Gal-Azo-SH and (B) *trans*-Man-Azo-SH.

S2. Additional Figures

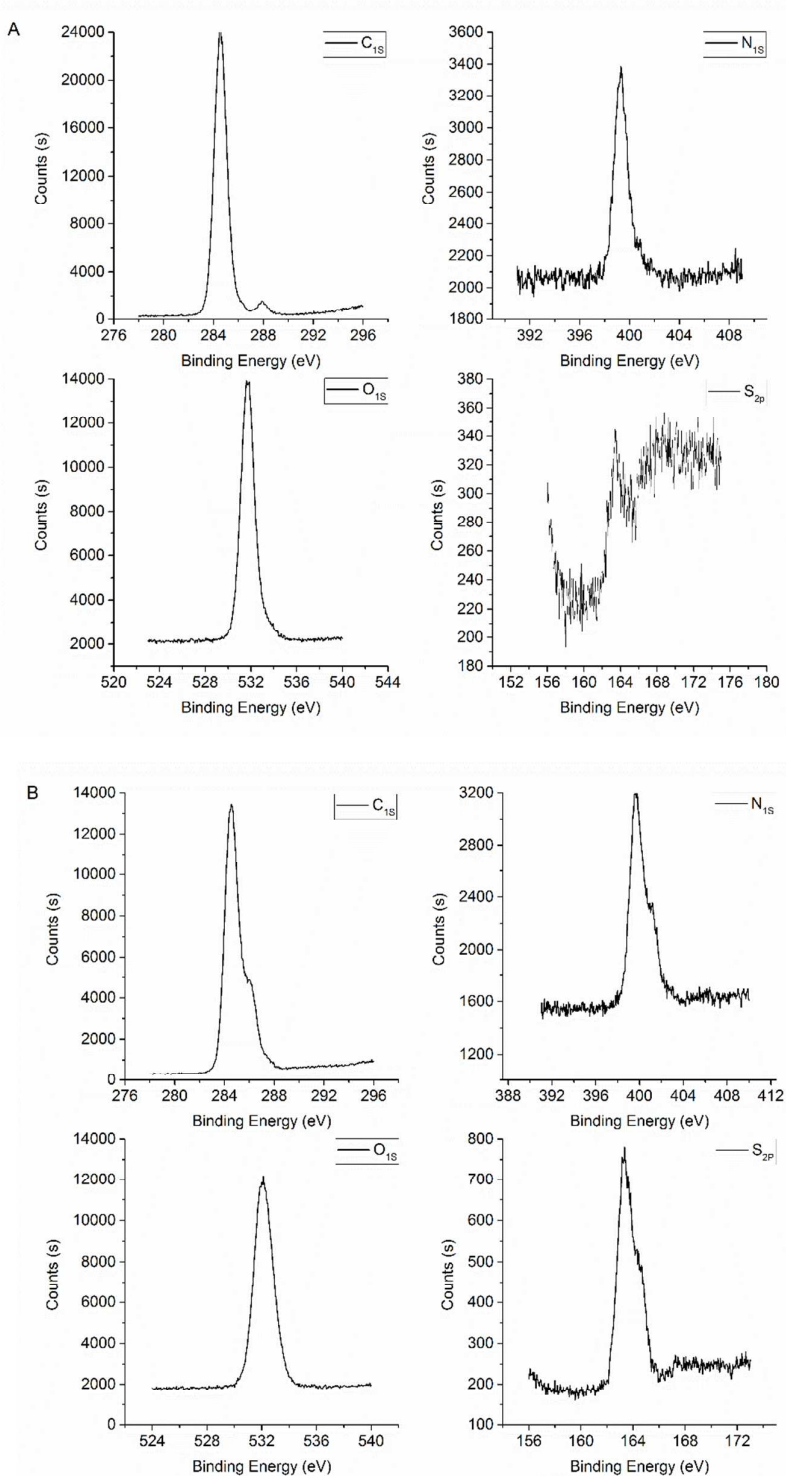


Figure S3. High-resolution XPS spectra of C_{1s}, N_{1s}, O_{1s}, and S_{2p} for *trans*-Gal-Azo-SAM (A) and *trans*-Man-Azo-SAM (B) on the gold surface. The N_{1s},

O_{1s} , and S_{2p} peaks for *trans*-Gal-Azo-SAM (A) were measured at 399.74 eV, 531.71 eV and 163.09 eV, respectively. The N_{1s} , O_{1s} , and S_{2p} peaks for *trans*-Man-Azo-SAM (B) were measured at 399.81 eV, 532.08 eV and 163.89 eV, respectively. XPS spectra were measured on a Thermo Scientific EscaLab 250Xi X-ray photoelectron spectrometer equipped with a Al K Alpha source ($h\nu = 1486.7$ eV). The XPS binding energy was calibrated with respect to the peak position of C_{1s} at 284.7 eV.

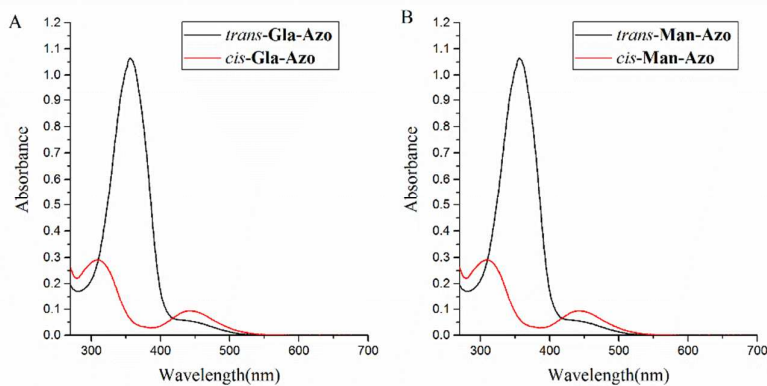


Figure S4. Photo-isomerization UV/Vis spectra of **Gal-Azo-SH** (A) and **Man-Azo-SH** (B) (4.0×10^{-5} mol L⁻¹ in DMSO).

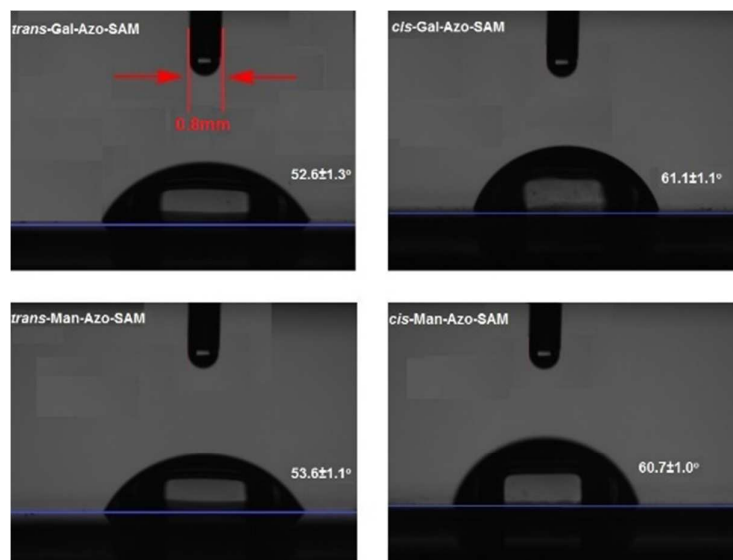


Figure S5. Images of the static water contact angles on the *trans/cis*-Gal-Azo-SH and *trans/cis*-Man-Azo-SH anchored on gold substrates. The blue lines indicate the surface plane. The diameter of the syringe needle is 0.8 mm.

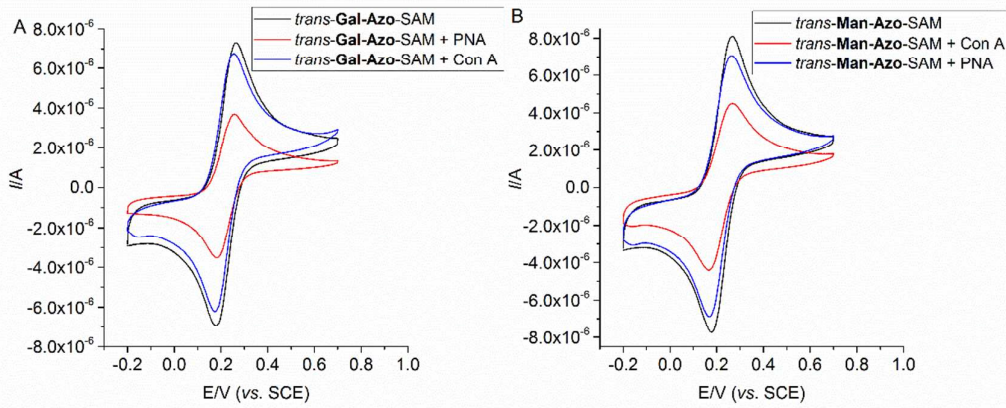


Figure S6. Cyclic voltammetry (CV) plots of (A) *trans*-Gal-Azo-SAM and (B) *trans*-Man-Azo-SAM upon addition of 7 μ M specific and non-specific protein (1.0 mM $[\text{Fe}(\text{CN})_6]^{3-/4-}$ + 0.1 M KCl).

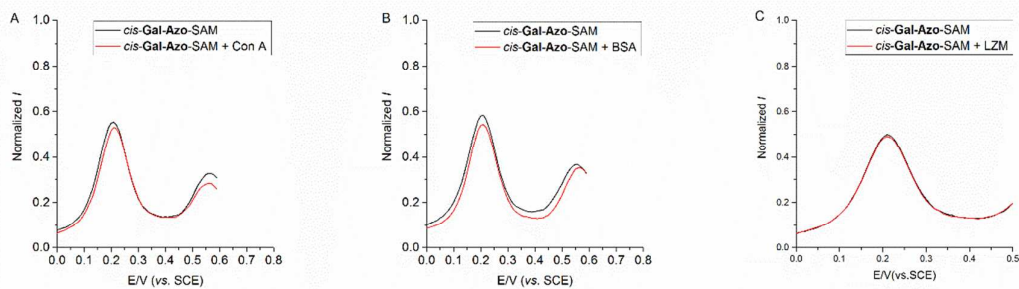


Figure S7. Differential pulse voltammetry (DPV) plots of *cis*-Gal-Azo-SAM upon addition of 7 μ M various non-specific protein (1.0 mM $[\text{Fe}(\text{CN})_6]^{3-/4-}$ + 0.1 M KCl): (A) Con A, (B) Bovine serum albumin (BSA) and (C) Lysozyme (LZM).

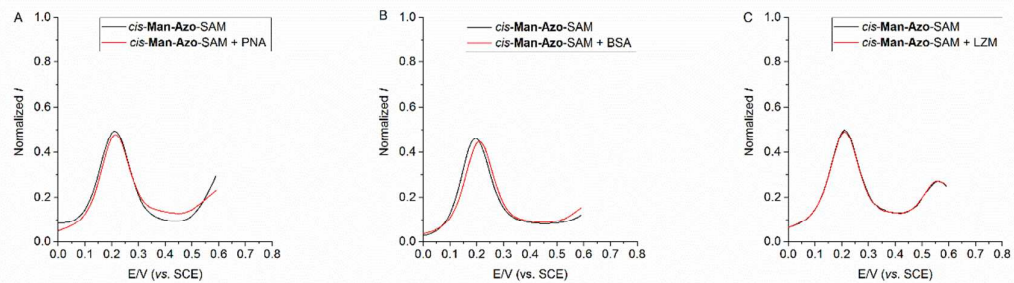


Figure S8. Differential pulse voltammetry (DPV) plots of *cis*-Man-Azo-SAM upon addition of 7 μ M various non-specific protein (1.0 mM $[\text{Fe}(\text{CN})_6]^{3-/4-}$ + 0.1 M KCl): (A) PNA, (B) Bovine serum albumin (BSA) and (C) Lysozyme (LZM).

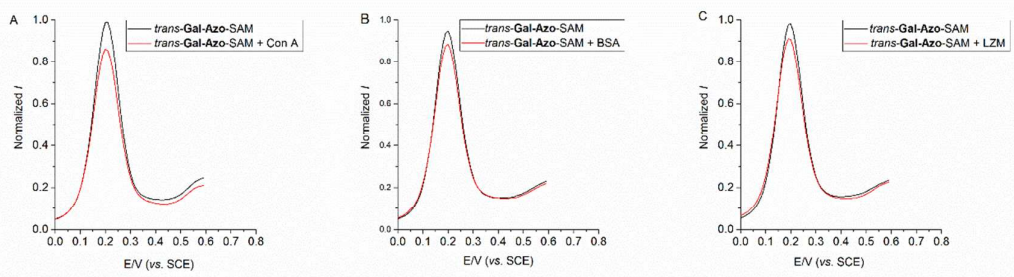


Figure S9. Differential pulse voltammetry (DPV) plots of **trans-Gal-Azo-SAM** upon addition of 7 μM various non-specific protein (1.0 mM $[\text{Fe}(\text{CN})_6]^{3-/4-}$ + 0.1 M KCl): (A) Con A, (B) Bovine serum albumin (BSA) and (C) Lysozyme (LZM).

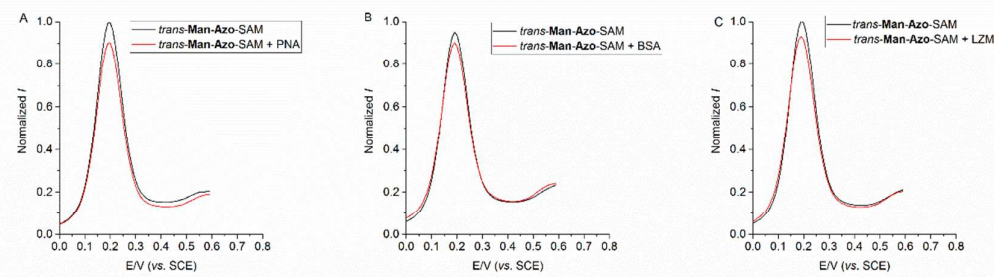


Figure S10. Differential pulse voltammetry (DPV) plots of **trans-Man-Azo-SAM** upon addition of 7 μM various non-specific protein (1.0 mM $[\text{Fe}(\text{CN})_6]^{3-/4-}$ + 0.1 M KCl): (A) PNA, (B) Bovine serum albumin (BSA) and (C) Lysozyme (LZM).

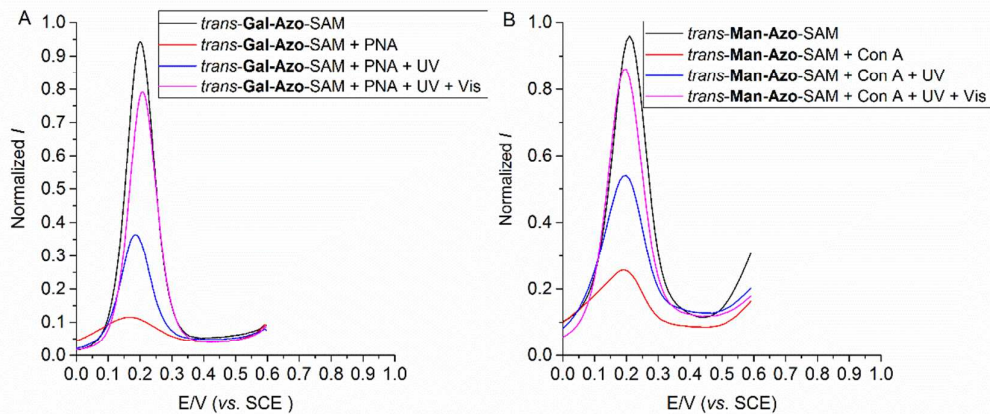


Figure S11. Differential pulse voltammetry (DPV) response of the photo-reversibility of (A) **Gal-Azo-SAM** upon the addition of 7 μM PNA (1.0 mM $[\text{Fe}(\text{CN})_6]^{3-/4-}$ + 0.1 M KCl) and (B) **Man-Azo-SAM** upon the addition of 7 μM Con A (1.0 mM $[\text{Fe}(\text{CN})_6]^{3-/4-}$ + 0.1 M KCl).

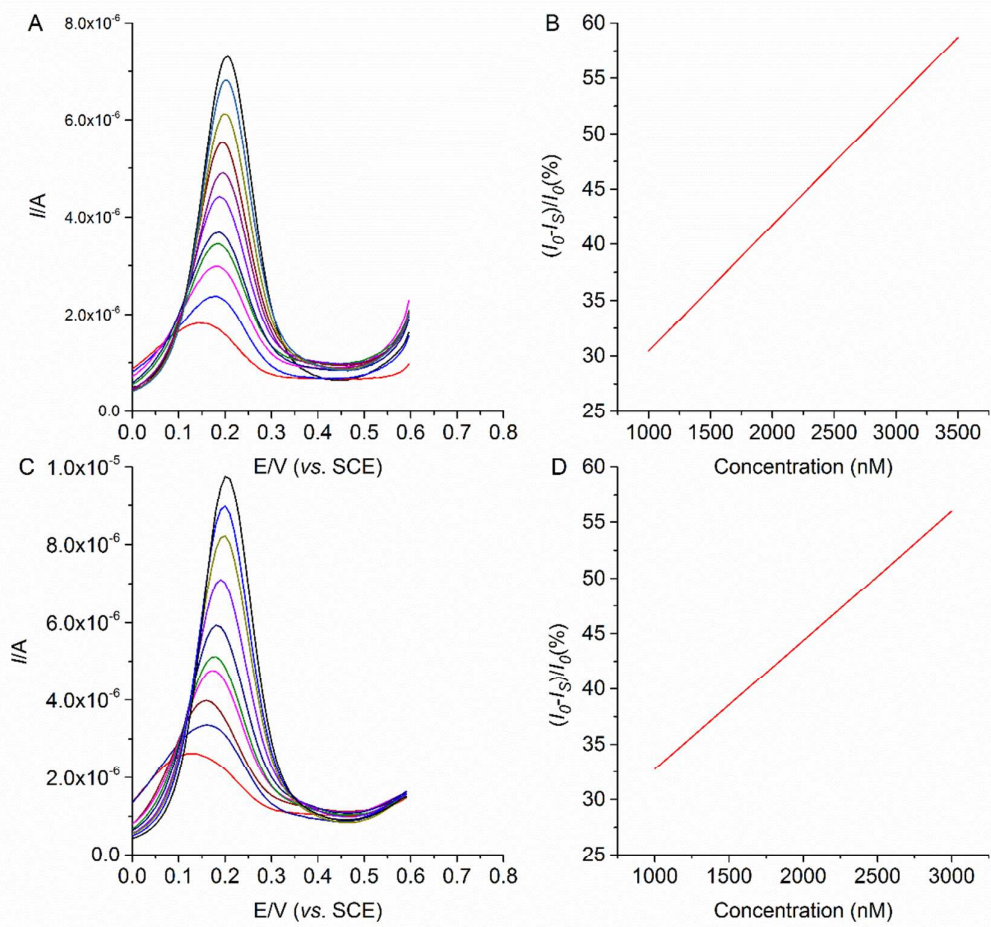


Figure S12. Differential pulse voltammetry (DPV) response of (A) *trans*-Gal-Azo-SAM upon the addition of various concentrations of PNA ranging from 0.1 to 10 μM (1.0 mM $[\text{Fe}(\text{CN})_6]^{3/4-}$ + 0.1 M KCl) and (C) *trans*-Man-Azo-SAM upon the addition of various concentrations of Con A ranging from 0.1 to 10 μM (1.0 mM $[\text{Fe}(\text{CN})_6]^{3/4-}$ + 0.1 M KCl). Plotting of protein sensitivity $(I_0 - I_S)/I_0$ (where I_S and I_0 are the current intensity in the presence and absence of a specific protein, respectively) of *trans*-Gal-Azo-SAM (B) and *trans*-Man-Azo-SAM (D) as a function of protein concentration.

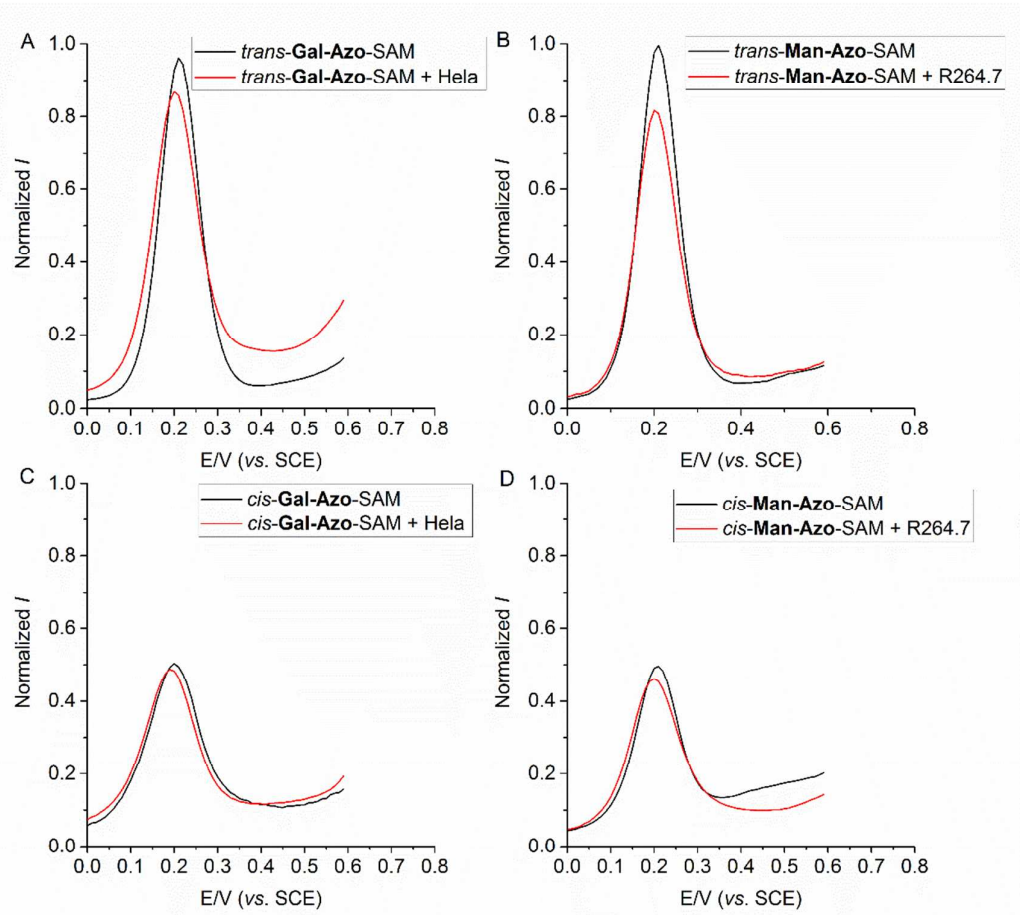


Figure S13. Differential pulse voltammetry (DPV) response of *trans/cis*-Gal-Azo-SAM (A and C) upon the addition of 10,0000 cell mL⁻¹ Hela (1.0 mM [Fe(CN)₆]^{3-/4-} + 0.1 M KCl) and *trans/cis*-Man-Azo-SAM (B and D) upon addition of 10,0000 cell mL⁻¹ of R264.7 (1.0 mM [Fe(CN)₆]^{3-/4-} + 0.1 M KCl).

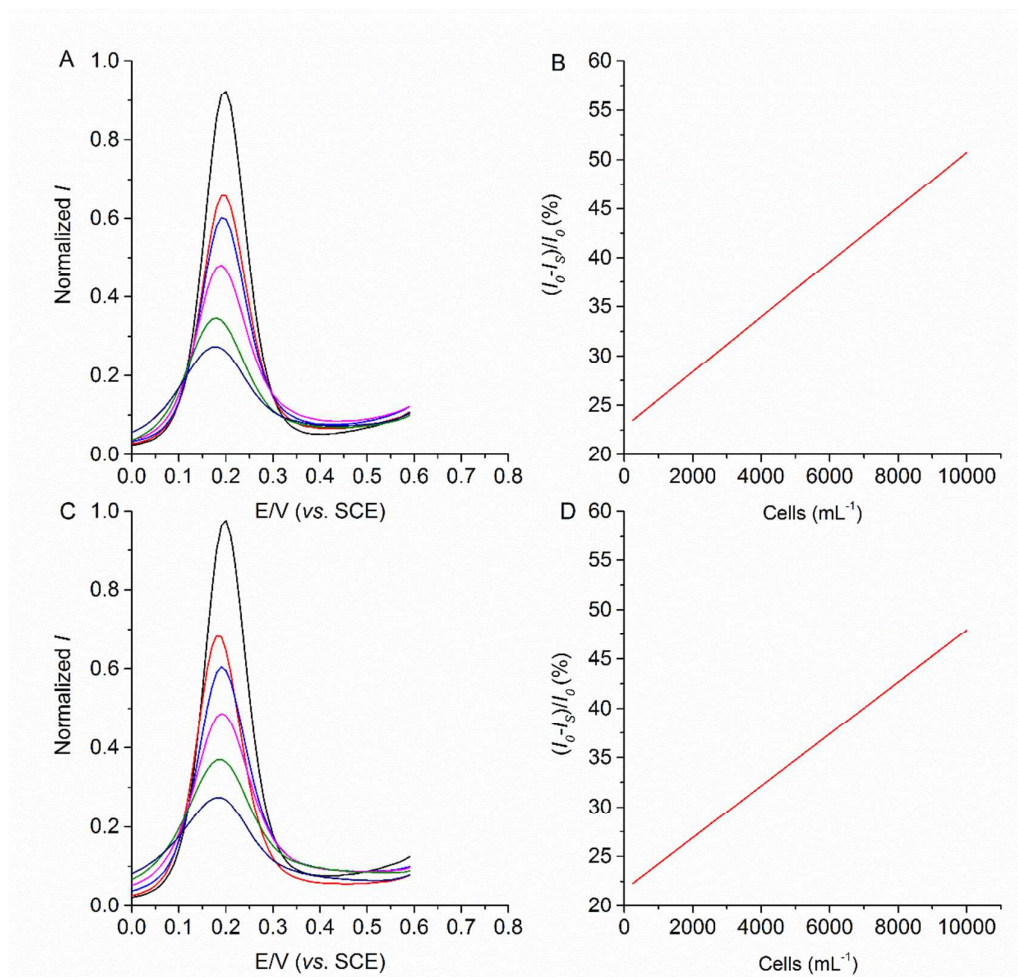


Figure S14. Differential pulse voltammetry (DPV) response of (A) *trans*-Gal-Azo-SAM upon the addition of various concentrations of Hep-G2 ranging from top to bottom: 0, 5000, 10000, 100000 and 500000 cells mL^{-1} (1.0 mM $[\text{Fe}(\text{CN})_6]^{3-/4-}$ + 0.1 M KCl) and (C) *trans*-Man-Azo-SAM upon the addition of various concentrations of M2 ranging from top to bottom: 0, 5000, 10000, 100000 and 500000 cells mL^{-1} (1.0 mM $[\text{Fe}(\text{CN})_6]^{3-/4-}$ + 0.1 M KCl). Plotting of cells sensitivity $(I_0 - I_S)/I_0$ (where I_S and I_0 are the current intensity in the presence and absence of cells respectively) of *trans*-Gal-Azo-SAM (B) and *trans*-Man-Azo-SAM (D) as a function of cells concentration.

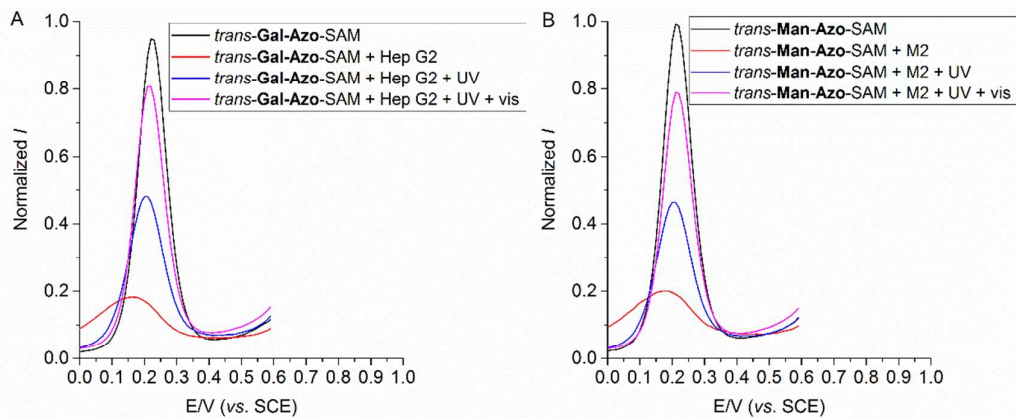


Figure S15. Differential pulse voltammetry (DPV) response of the photo-reversibility of (A) **Gal-Azo-SAM** upon the addition of 10,0000 cell mL⁻¹ Hep-G2 (1.0 mM [Fe(CN)₆]^{3-/4-} + 0.1 M KCl) and (B) **Man-Azo-SAM** upon the addition of 10,0000 cell mL⁻¹ M2 (1.0 mM [Fe(CN)₆]^{3-/4-} + 0.1 M KCl).

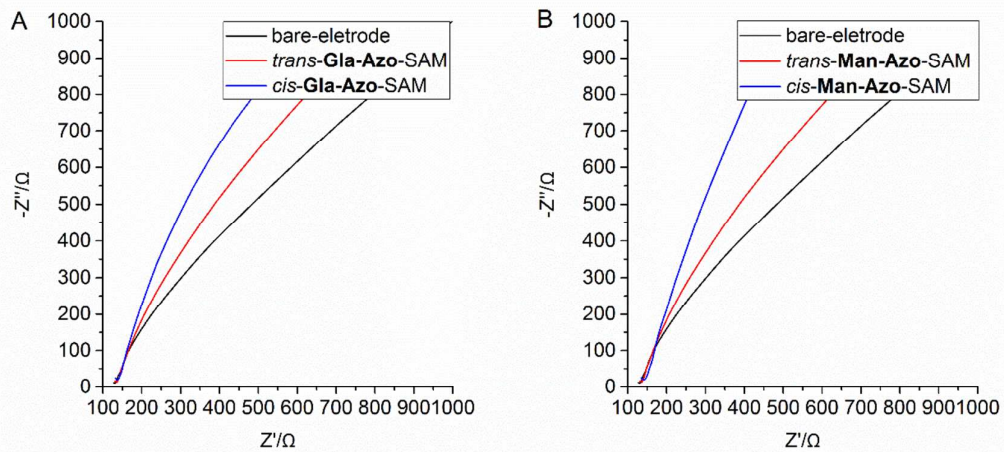


Figure S16. Faradaic impedance spectroscopy plots of **Gal-Azo-SH** (A) and **Man-Azo-SH** (B) modified electrode monolayers after UV/Vis irradiation (1.0 mM [Fe(CN)₆]^{3-/4-} + 0.1 M KCl).

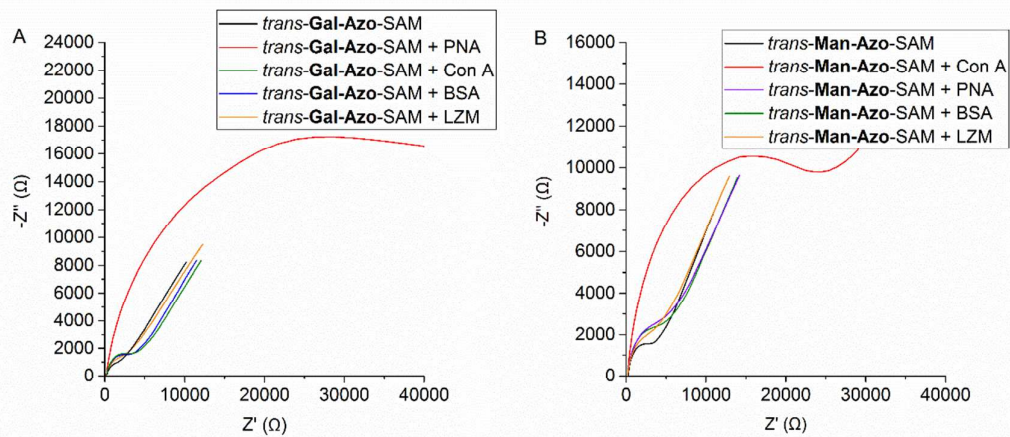


Figure S17. Faradaic impedance spectroscopy plots of (A) *trans*-**Gal-Azo** SAM and (B) *trans*-**Man-Azo** SAM upon addition of 7 μM various specific and non-specific protein (1.0 mM $[\text{Fe}(\text{CN})_6]^{3-/4-}$ + 0.1 M KCl).

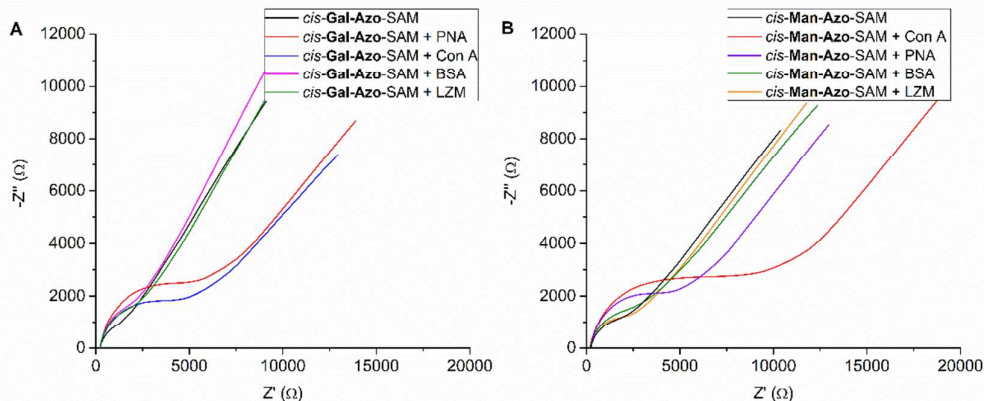


Figure S18. Faradaic impedance spectroscopy plots of (A) *cis*-**Gal-Azo** SAM and (B) *cis*-**Man-Azo** SAM upon addition of 7 μM various specific and non-specific protein (1.0 mM $[\text{Fe}(\text{CN})_6]^{3-/4-}$ + 0.1 M KCl).

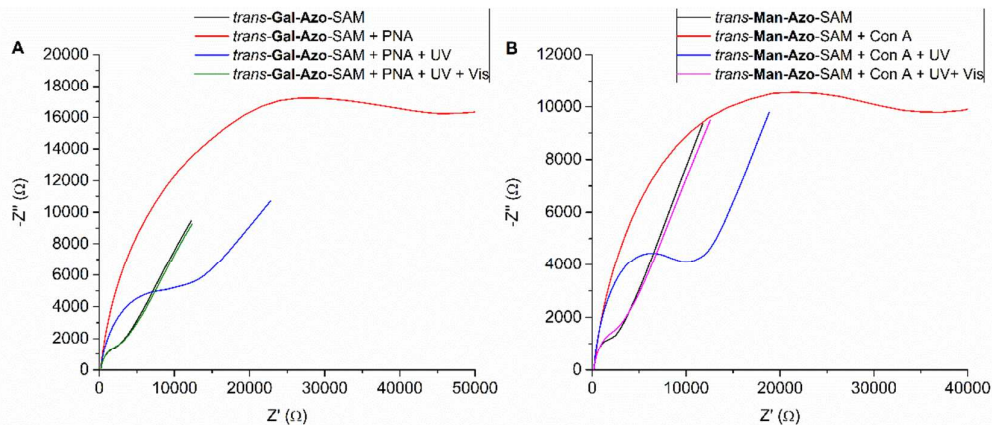


Figure S19. Faradaic impedance spectroscopy response of the photo-reversibility of

(A) *trans*-Gal-Azo-SAM upon the addition of 7 μM PNA (1.0 mM $[\text{Fe}(\text{CN})_6]^{3-/4-}$ + 0.1 M KCl) and (B) *trans*-Man-Azo-SAM upon the addition of 7 μM Con A (1.0 mM $[\text{Fe}(\text{CN})_6]^{3-/4-}$ + 0.1 M KCl).

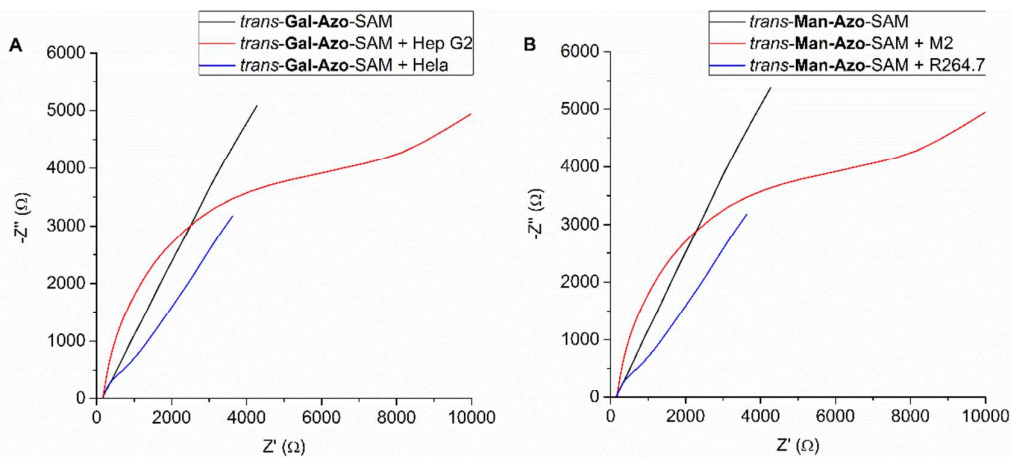


Figure S20. Faradaic impedance spectroscopy plots of (A) *trans*-Gal-Azo SAM and (B) *trans*-Man-Azo SAM upon addition of 100000 cells mL^{-1} various specific and non-specific cells (1.0 mM $[\text{Fe}(\text{CN})_6]^{3-/4-}$ + 0.1 M KCl).

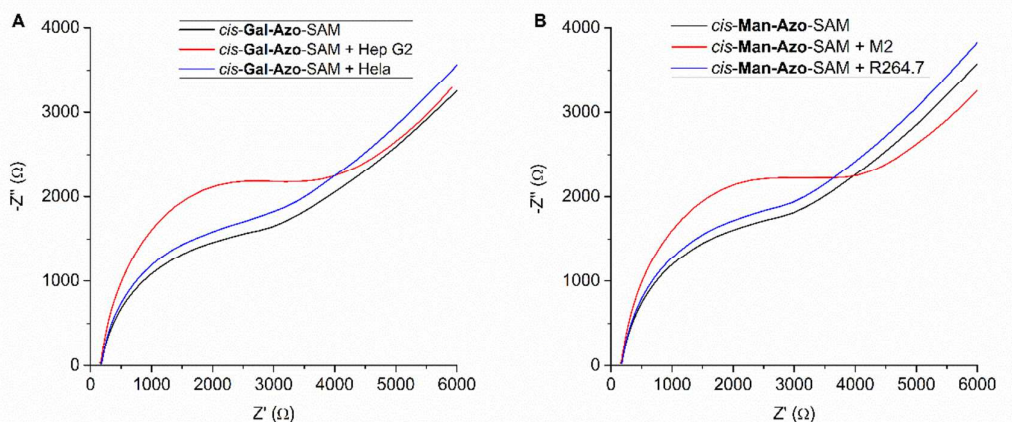


Figure S21. Faradaic impedance spectroscopy plots of (A) *cis*-Gal-Azo SAM and (B) *cis*-Man-Azo SAM upon addition of 100000 cells mL^{-1} various specific and non-specific cells (1.0 mM $[\text{Fe}(\text{CN})_6]^{3-/4-}$ + 0.1 M KCl).

References:

- (1) Chandrasekaran, V.; Lindhorst, T. K. Sweet Switches: Azobenzene Glycoconjugates Synthesized by Click Chemistry. *Chem. Commun.* **2012**, 48, 7519–7521.
- (2) Zhu, L. L.; Zhang, D.; Qu, D. H.; Wang, Q. C.; Ma, X.; Tian, H. Dual-Controllable

Stepwise Supramolecular Interconversions. *Chem. Commun.* **2010**, *46*, 2587–2589.